

Characterisation of Low Frequency Gravitational Waves from Dual RF Coaxial-Cable Detector: Fractal Textured Dynamical 3-Space

Reginald T. Cahill

Progress in Physics **3**, 3-10, 2012

School of Chemical and Physical Sciences, Flinders University, Adelaide 5001, Australia

E-mail: Reg.Cahill@flinders.edu.au

Experiments have revealed that the Fresnel drag effect is not present in RF coaxial cables, contrary to a previous report. This enables a very sensitive, robust and compact detector, that is 1st order in v/c and using one clock, to detect the dynamical space passing the earth, revealing the sidereal rotation of the earth, together with significant wave/turbulence effects. These are “gravitational waves”, and previously detected by Cahill 2006, using an Optical-Fibre - RF Coaxial Cable Detector, and Cahill 2009, using a preliminary version of the Dual RF Coaxial Cable Detector. The gravitational waves have a $1/f$ spectrum, implying a fractal textured structure to dynamical 3-space.

1 Introduction

Data from a new gravitational wave experiment is reported¹, revealing a fractal textured 3-space, flowing past the earth at ~ 500 km/s. The wave/turbulence or “gravitational waves” have a significant magnitude, and are now known to have been detected numerous times over the last 125 years. The detector uses a single clock with RF EM waves propagating through dual coaxial cables, and is 1st order in v/c . The detector is sensitive, simple to operate, robust and compact. It uses the surprising discovery that there is no Fresnel drag effect in coaxial cables, whereas there is in gases, optical fibres, liquids etc. Data from an analogous detector using optical fibres and single coaxial cables was reported in 2006 [1, 2]. Because of the discovery reported herein that detector calibration has now been correctly redetermined. Results from Michelson-Morley [3, 4], Miller [5], Torr and Kolen [6] and DeWitte [7], are now in remarkable agreement with the velocity of absolute motion of the earth determined from NASA spacecraft earth-flyby Doppler shift data [8, 9], all revealing a light/EM speed anisotropy of some 486km/s in the direction $RA=4.29^h$, $Dec=-75.0^\circ$: that speed is $\sim 300,000-500$ km/s for radiation travelling in that direction, and $\sim 300,000+500$ km/s travelling in the opposite, northerly, direction: a significant observed anisotropy that physics has ignored. The actual daily average velocity varies with days of the year because of the orbital motion of the earth - the aberration effect discovered by Miller, but shows fluctuations over all time scales.

In 2002 it was discovered that the Michelson-Morley 1887 light-speed anisotropy experiment, using the interferometer in gas mode, had indeed detected anisotropy, by taking account of both the Lorentz length contraction effect for the interferometer arms, and the refractive index effect of the air in the light paths [3, 4]. These gas-mode interferometer experiments show

the difference between Lorentzian Relativity (LR) and Special Relativity (SR). In LR the length contraction effect is caused by motion of a rod, say, through the dynamical 3-space, whereas in SR the length contraction is only a perspective effect, supposedly occurring only when the rod is moving relative to an observer. This was further clarified when an exact mapping between Galilean space and time coordinates and the Minkowski-Einstein spacetime coordinates was recently discovered [10].

The Michelson interferometer, having the calibration constant $k^2 = (n^2 - 1)(n^2 - 2)$ where n is the refractive index of the light-path medium, has zero sensitivity to EM anisotropy and gravitational waves when operated in vacuum-mode ($n = 1$). Fortunately the early experiments had air present in the light paths². A very compact and cheap Michelson interferometric anisotropy and gravitational wave detector may be constructed using optical fibres [11], but for most fibres $n \approx \sqrt{2}$ near room temperature, and so needs to be operated at say $0^\circ C$. The $(n^2 - 2)$ factor is caused by the Fresnel drag [12]. The detection of light speed anisotropy - revealing a flow of space past the detector, is now entering an era of precision measurements, as reported herein. These are particularly important because experiments have shown large turbulence effects in the flow, and are beginning to characterise this turbulence. Such turbulence can be shown to correspond to what are, conventionally, known as gravitational waves, although not those implied by General Relativity, but more precisely are revealing a fractal structure to dynamical 3-space.

²Michelson and Morley implicitly assumed that $k^2 = 1$, which considerably overestimated the sensitivity of their detector by a factor of ~ 1700 (air has $n = 1.00029$). This error led to the invention of “spacetime” in 1905. Miller avoided any assumptions about the sensitivity of his detector, and used the earth orbit effect to estimate the calibration factor k^2 from his data, although even that is now known to be incorrect: the sun 3-space inflow component was unknown to Miller. It was only in 2002 that the design flaw in the Michelson interferometer was finally understood [3, 4].

¹This report is from the Gravitational Wave Detector Project at Flinders University.

2 Fresnel Drag

The detection and characterisation of these wave/turbulence effects requires only the development of small and cheap detectors, as these effects are large. However in all detectors the EM signals travel through a dielectric, either in bulk or optical fibre or through RF coaxial cables. For this reason it is important to understand the so-called Fresnel drag effect. In optical fibres the Fresnel drag effect has been established, as this is important in the operation of Sagnac optical fibre gyroscopes, for only then is the calibration independent of the fibre refractive index, as observed. The Fresnel drag effect is a phenomenological formalism that characterises the effect of the absolute motion of the propagation medium, say a dielectric, upon the speed of the EM radiation relative to that medium.

The Fresnel drag expression is that a dielectric in absolute motion through space at speed v , relative to space itself, causes the EM radiation to travel at speed

$$V(v) = \frac{c}{n} + v \left(1 - \frac{1}{n^2}\right) \quad (1)$$

wrt the dielectric, when V and v have the same direction. Here n is the dielectric refractive index. The 2nd term is known as the Fresnel drag, appearing to show that the moving dielectric “drags” the EM radiation, although this is a misleading interpretation; see [13] for a derivation³. If the Fresnel drag is always applicable then, as shown herein, a 1st order in v/c detector requires two clocks, though not necessarily synchronised, but requiring a rotation of the detector arm to extract the v -dependent term. However, as we show herein, if the Fresnel drag is not present in RF coaxial cables, then a detector 1st order in v/c and using one clock, can detect and characterise the dynamical space. In [13] it was incorrectly concluded that the Fresnel effect was present in RF coaxial cables, for reasons related to the temperature effects, and discussed later.

3 Dynamical 3-Space

We briefly outline the dynamical modelling of 3-space. It involves the space velocity field $\mathbf{v}(\mathbf{r}, t)$, defined relative to an observer’s frame of reference.

$$\nabla \cdot \left(\frac{\partial \mathbf{v}}{\partial t} + (\mathbf{v} \cdot \nabla) \mathbf{v} \right) + \frac{\alpha}{8} \left((\text{tr} D)^2 - \text{tr}(D^2) \right) + \dots = -4\pi G \rho \quad (2)$$

$\nabla \times \mathbf{v} = \mathbf{0}$ and $D_{ij} = \partial v_i / \partial x_j$. The velocity field \mathbf{v} describes classically the time evolution of the substratum quantum foam. The bore hole g anomaly data has revealed $\alpha = 1/137$, the fine structure constant. The matter acceleration is found by determining the trajectory of a quantum matter wavepacket. This is

³The Fresnel Drag in (1) can be “derived” from the Special Relativity velocity-addition formula, but there v is the speed of the dielectric wrt to the observer, and as well common to both dielectrics and coaxial cables.

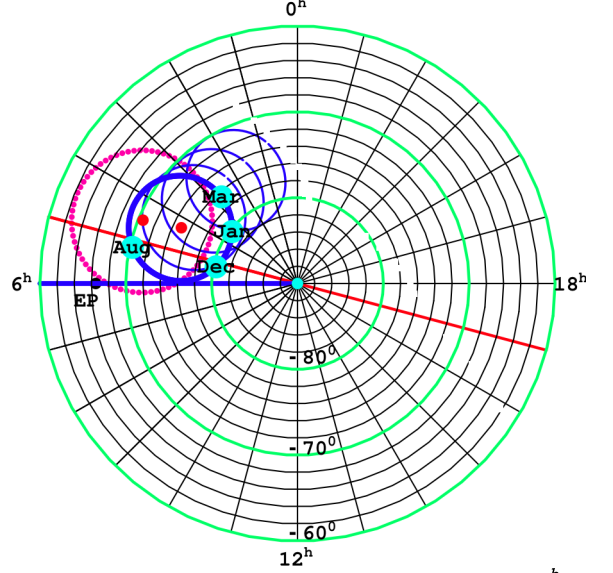


Fig. 1: South celestial pole region. The dot (red) at RA=4.29^h, Dec=-75°, and with speed 486km/s, is the direction of motion of the solar system through space determined from NASA spacecraft earth-flyby Doppler shifts [9], revealing the EM radiation speed anisotropy. The thick (blue) circle centred on this direction is the observed velocity direction for different days of the year, caused by earth orbital motion and sun 3-space inflow. The corresponding results from Miller gas-mode interferometer are shown by 2nd dot (red) and its aberration circle (red dots) [5]. For March the velocity is RA=2.75^h, Dec=-76.6°, and with speed 499.2km/s, see Table 2 of [9]. The thinner blue aberration circles relate to determination of earth 3-space inflow speed, see [9].

most easily done by maximising the proper travel time τ :

$$\tau = \int dt \sqrt{1 - \frac{\mathbf{v}_R^2(\mathbf{r}_o(t), t)}{c^2}} \quad (3)$$

where $\mathbf{v}_R(\mathbf{r}_o(t), t) = \mathbf{v}_o(t) - \mathbf{v}(\mathbf{r}_o(t), t)$, is the velocity of the wave packet, at position $\mathbf{r}_o(t)$, wrt the local space - a neo-Lorentzian Relativity effect. This ensures that quantum waves propagating along neighbouring paths are in phase, and so interfere constructively. This maximisation gives the quantum matter geodesic equation for $\mathbf{r}_o(t)$

$$\mathbf{g} = \frac{\partial \mathbf{v}}{\partial t} + (\mathbf{v} \cdot \nabla) \mathbf{v} + (\nabla \times \mathbf{v}) \times \mathbf{v}_R - \frac{\mathbf{v}_R}{1 - \frac{\mathbf{v}_R^2}{c^2}} \frac{1}{2} \frac{d}{dt} \left(\frac{\mathbf{v}_R^2}{c^2} \right) + \dots \quad (4)$$

with $\mathbf{g} \equiv d\mathbf{v}_o/dt = d^2\mathbf{r}_o/dt^2$. The 1st term in \mathbf{g} is the Euler space acceleration \mathbf{a} , the 2nd term explains the Lense-Thirring effect, when the vorticity is non-zero, and the last term explains the precession of orbits. While the velocity field has been repeatedly detected since the Michelson-Morley 1887 experiment, the best detection has been using the spacecraft earth-flyby Doppler shift data [9], see Fig.1. The above reveals gravity to be an emergent phenomenon where quantum matter waves are refracted by the time dependent and inhomogeneous 3-space velocity field. The α -term in (2) explains the so-called “dark matter” effects: if $\alpha \rightarrow 0$ and $v_R/c \rightarrow 0$ we derive New-

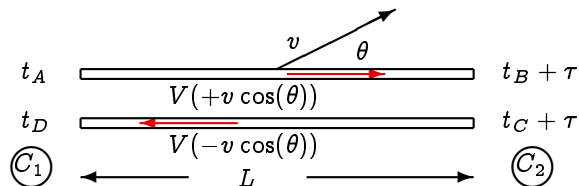


Fig. 2: Schematic layout for measuring the one-way speed of light in either free-space, optical fibres or RF coaxial cables, without requiring the synchronisation of the clocks C_1 and C_2 : here τ is the unknown offset time between the clocks. V is the speed of EM radiation wrt the apparatus, with or without the Fresnel drag in (1), and v is the speed of the apparatus through space, in direction θ . DeWitte used this technique in 1991 with 1.5km RF cables and Cesium atomic clocks [7]. In comparison with data from spacecraft earth-flyby Doppler shifts [9] this experiments confirms that there is no Fresnel drag effect in RF coaxial cables.

tonian gravity, for then $\nabla \cdot \mathbf{g} = -4\pi G\rho$ [12]. Note that the relativistic term in (4) arises from the quantum matter dynamics - not from the space dynamics.

4 Gravitational Waves: Dynamical Fractal 3-Space

Eqn.(3) for the elapsed proper time maybe written in differential form as

$$d\tau^2 = dt^2 - \frac{1}{c^2} (d\mathbf{r}(t) - \mathbf{v}(\mathbf{r}(t), t) dt)^2 = g_{\mu\nu}(x) dx^\mu dx^\nu \quad (5)$$

which introduces a curved spacetime metric $g_{\mu\nu}$ for which the geodesics are the quantum matter trajectories when freely propagating through the dynamical 3-space. Gravitational wave are traditionally thought of as “ripples” in the space-time metric $g_{\mu\nu}$. But the discovery of the dynamical 3-space means that they are more appropriately understood to be turbulence effects of the dynamical 3-space vector \mathbf{v} , because it is \mathbf{v} that is directly detectable, whereas $g_{\mu\nu}$ is merely an induced mathematical artefact. When the matter density $\rho = 0$, (2) will have a time-dependent fractal structure solutions, as there is no length scale. The wave/turbulence effects reported herein confirm that prediction, see Fig.9.

5 First Order in v/c Speed of EMR Experiments

Fig.2 shows the arrangement for measuring the one-way speed of light, either in vacuum, a dielectric, or RF coaxial cable. It is usually argued that one-way speed of light measurements are not possible because the clocks C_1 and C_2 cannot be synchronised. However this is false, and at the same time shows an important consequence of (1). In the upper part of Fig.2 the actual travel time t_{AB} from A to B is determined by

$$V(v \cos(\theta))t_{AB} = L + v \cos(\theta)t_{AB} \quad (6)$$

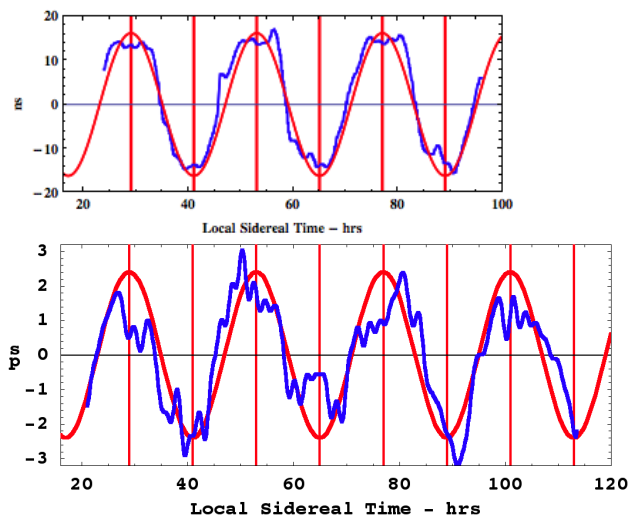


Fig. 3: Top: Data from the 1991 DeWitte NS horizontal coaxial cable experiment, $L = 1.5\text{km}$, $n = 1.5$, using the arrangement shown in Fig.2. The time variation of $\sim 28\text{ns}$ is consistent with the Doppler shift results with speed 500km/s , but using $\text{Dec} = -65^\circ$: the month for this data is unknown, and the vertical red lines are at $\text{RA} = 5^h$. If a Fresnel drag effect is included the speed would have to be 1125km/s , in disagreement with the Doppler shift data, demonstrating that there is no Fresnel drag in coaxial cables. Bottom: Dual coaxial cable detector data from May 2009 using the technique in Fig.6 and without looping: $L = 20\text{m}$, Doppler shift data predicts $\text{Dec} = -77^\circ$, $v = 480\text{km/s}$ giving a sidereal dynamic range of 5.06ps , very close to that observed. The vertical red lines are at $\text{RA} = 5^h$. In both data sets we see the earth sidereal rotation effect together with significant wave/turbulence effects.

where the 2nd term comes from the end B moving an additional distance $v \cos(\theta)t_{AB}$ during time interval t_{AB} . Then

$$t_{AB} = \frac{L}{V(v \cos(\theta)) - v \cos(\theta)} = \frac{nL}{c} + \frac{v \cos(\theta)L}{c^2} + \dots \quad (7)$$

$$t_{CD} = \frac{L}{V(v \cos(\theta)) + v \cos(\theta)} = \frac{nL}{c} - \frac{v \cos(\theta)L}{c^2} + \dots \quad (8)$$

on using (1), i.e. assuming the validity of the Fresnel effect, and expanding to 1st order in v/c . However if there is no Fresnel drag effect then we obtain

$$t_{AB} = \frac{L}{V(v \cos(\theta)) - v \cos(\theta)} = \frac{nL}{c} + \frac{v \cos(\theta)Ln^2}{c^2} + \dots \quad (9)$$

$$t_{CD} = \frac{L}{V(v \cos(\theta)) + v \cos(\theta)} = \frac{nL}{c} - \frac{v \cos(\theta)Ln^2}{c^2} + \dots \quad (10)$$

The important observation is that the v/c terms are independent of the dielectric refractive index n in (7) and (8), but have an n^2 dependence in (9) and (10), in the absence of the Fresnel drag effect.

If the clocks are not synchronised then t_{AB} is not known, but by changing direction of the light path, that is varying θ , the magnitude of the 2nd term may be separated from the magnitude of the 1st term, and v and its direction determined. The

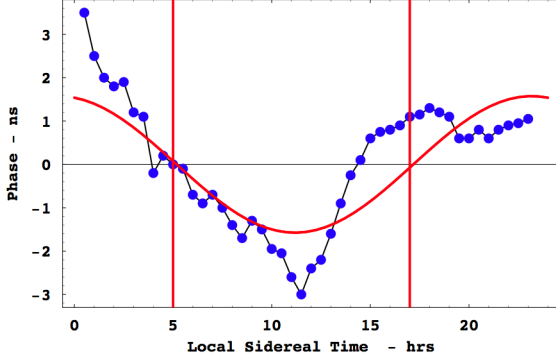


Fig. 4: Data from the 1981 Torr-Kolen experiment at Logan, Utah [6]. The data shows variations in travel times (ns), for local sidereal times, of an RF signal travelling through 500 m of coaxial cable orientated in an EW direction. The red curve is sidereal effect prediction for February, for a 3-space speed of 480 km/s from the direction, RA=5^h, Dec=-70°.

clocks may then be synchronised. For a small detector the change in θ can be achieved by a direct rotation. Results (7) and (8), or (9) and (10), have been exploited in various detector designs.

6 DeWitte 1st Order in v/c Detector

The DeWitte $L = 1.5$ km RF coaxial cable experiment, Brussels 1991, was a double 1st order in v/c detector, using the scheme in Fig.2, and employing 3 Caesium atomic clocks at each end, and overall measuring $t_{AB} - t_{CD}$. The orientation was NS and rotation was achieved by that of the earth [7].

$$t_{AB} - t_{CD} = \frac{2v \cos(\theta) L n^2}{c^2} \quad (11)$$

The dynamic range of $\cos(\theta)$ is $2 \sin(\lambda - \beta) \cos(\delta)$, caused by the earth rotation, where λ is the latitude of the detector location, β is the local inclination to the horizontal, here $\beta = 0$, and δ is the declination of \mathbf{v} . The data shows remarkable agreement with the velocity vector from the flyby Doppler shift data, see Fig.3. However if there is Fresnel drag in the coaxial cables, there would be no n^2 factor in (11), and the DeWitte data would give a much larger speed $v = 1125$ km/s, in strong disagreement with the flyby data.

7 Torr and Kolen 1st Order in v/c Detector

A one-way coaxial cable experiment was performed at the Utah University in 1981 by Torr and Kolen [6]. This involved two Rb clocks placed approximately 500 m apart with a 5 MHz sinewave RF signal propagating between the clocks via a nitrogen filled coaxial cable buried in the ground and maintained

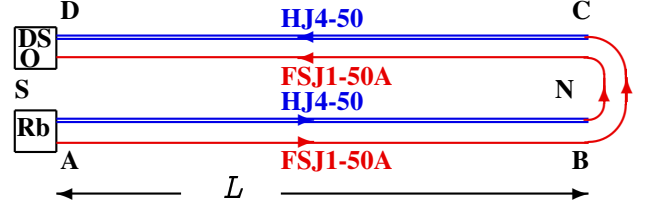


Fig. 6: Because Fresnel drag is absent in RF coaxial cables this dual cable setup, using one clock, is capable of detecting the absolute motion of the detector wrt to space, revealing the sidereal rotation effect as well as wave/turbulence effects. In the 1st trial of this detector this arrangement was used, with the cables laid out on a laboratory floor, and preliminary results are shown in Figs.3. In the new design the cables in each circuit are configured into 8 loops, as in Fig.5, giving $L = 8 \times 1.85 \text{ m} = 14.8 \text{ m}$. In [1] a version with optical fibres in place of the HJ4-50 coaxial cables was used, see Fig.11. There the optical fibre has a Fresnel drag effect while the coaxial cable did not. In that experiment optical-electrical converters were used to modulate/demodulate infrared light.

at a constant pressure of ~ 2 psi. Torr and Kolen observed variations in the one-way travel time, as shown in Fig.4 by the data points. The theoretical predictions for the Torr-Kolen experiment for a cosmic speed of 480 km/s from the direction, RA=5^h, Dec=-70°, as shown in Fig.4. The maximum/minimum effects occurred, typically, at the predicted times. Torr and Kolen reported fluctuations in both the magnitude, from 1 - 3 ns, and time of the maximum variations in travel time, just as observed in all later experiments, namely wave effects.

8 Dual RF Coaxial Cable Detector

The Dual RF Coaxial Cable Detector exploits the Fresnel drag anomaly, in that there is no Fresnel drag effect in RF coaxial cables. Then from (9) and (10) the round trip travel time is, see Fig.6,

$$t_{AB} + t_{CD} = \frac{(n_1 + n_2)L}{c} + \frac{v \cos(\theta)L(n_1^2 - n_2^2)}{c^2} + \dots \quad (12)$$

where n_1 and n_2 are the effective refractive indices for the two different RF coaxial cables, with two separate circuits to reduce temperature effects. Shown in Fig.5 is a photograph. The Andrews Phase Stabilised FSJ1-50A has $n_1 = 1.19$, while the HJ4-50 has $n_2 = 1.11$. One measures the travel time difference of two RF signals from a Rubidium frequency standard (Rb) with a Digital Storage Oscilloscope (DSO). In each circuit the RF signal travels one-way in one type of coaxial cable, and returns via a different kind of coaxial cable. Two circuits are used so that temperature effects cancel - if a temperature change alters the speed in one type of cable, and so the travel time, that travel time change is the same in both circuits, and cancels in the difference. The travel time difference of the two circuits at the DSO is

$$\Delta t = \frac{2v \cos(\theta)L(n_1^2 - n_2^2)}{c^2} + \dots \quad (13)$$

If the Fresnel drag effect occurred in RF coaxial cables, we would use (7) and (8) instead, and then the $n_1^2 - n_2^2$ term is

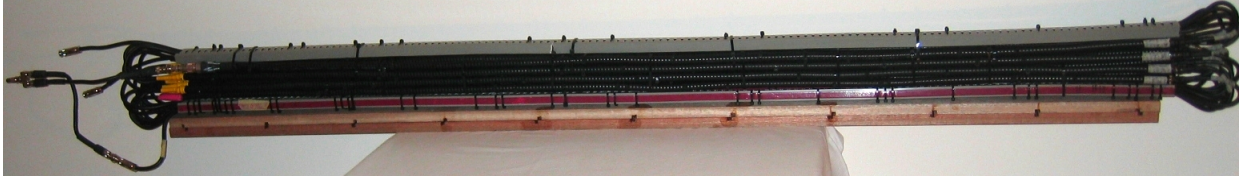


Fig. 5: Photograph of the RF coaxial cables arrangement, based upon $16 \times 1.85\text{m}$ lengths of phase stabilised Andrew HJ4-50 coaxial cable. These are joined to 16 lengths of phase stabilised Andrew FSJ1-50A cable, in the manner shown schematically in Fig.6. The 16 HJ4-50 coaxial cables have been tightly bound into a 4×4 array, so that the cables, locally, have the same temperature, with cables in one of the circuits embedded between cables in the 2nd circuit. This arrangement of the cables permits the cancellation of temperature differential effects in the cables. A similar array of the smaller diameter FSJ1-50A cables is located inside the grey-coloured conduit boxes.

replaced by 0, i.e. there is no 1st order term in v . That is contrary to the actual data in Figs.3 and 7.

The preliminary layout for this detector used cables laid out as in Fig.6, and the data is shown in Fig.3. In the compact design the Andrew HJ4-50 cables are cut into $8 \times 1.85\text{m}$ shorter lengths in each circuit, corresponding to a net length of $L = 8 \times 1.85 = 14.8\text{m}$, and the Andrew FSJ1-50A cables are also cut, but into longer lengths to enable joining. However the curved parts of the Andrew FSJ1-50A cables contribute only at 2nd order in v/c . The apparatus was horizontal, $\beta = 0$, and orientated NS, and used the rotation of the earth to change the angle θ . The dynamic range of $\cos(\theta)$, caused by the earth rotation only, is again $2 \sin(\lambda - \beta) \cos(\delta)$, where $\lambda = -35^\circ$ is the latitude of Adelaide. Inclining the detector at angle $\beta = \lambda$ removes the earth rotation effect, as now the detector arm is parallel to the earth's spin axis, permitting a more accurate characterisation of the wave effects.

9 Temperature Effects

The cable travel times and the DSO phase measurements are temperature dependent, and these effects are removed from the data, rather than attempt to maintain a constant temperature, which is impractical because of the heat output of the Rb clock and DSO. The detector was located in a closed room in which the temperature changed slowly over many days, with variations originating from changing external weather driven temperature changes. The temperature of the detector was measured, and it was assumed that the timing errors were proportional to changes in that one measured temperature. These timing errors were some 30ps, compared to the true signal of some 8ps. Because the temperature timing errors are much larger, the temperature induced $\Delta t = a + b\Delta T$ was fitted to the timing data, and the coefficients a and b determined. Then this Δt time series was subtracted from the data, leaving the actual required phase data. This is particularly effective as the temperature variations had a distinctive time signature. The resulting data is shown in Fig.8. In an earlier test for the Fresnel drag effect in RF coaxial cables [13] the technique for removing the temperature induced timing errors was inadequate, resulting in the wrong conclusion that there was Fresnel drag in RF coaxial cables.

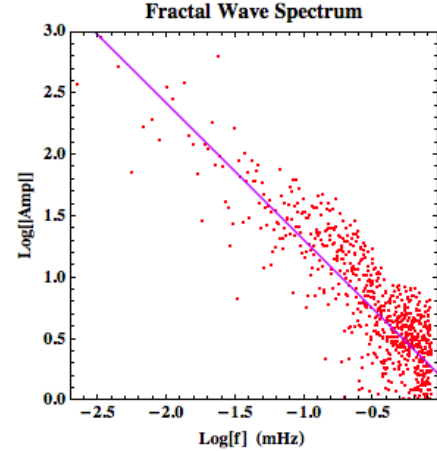


Fig. 7: Log-Log plot of the data (top) in Fig.7, with the straight line being $A \propto 1/f$, indicating a $1/f$ fractal wave spectrum. The interpretation for this is the 3-space structure shown in Fig.9.

10 Dual RF Coaxial Cable Detector: Data

The phase data, after removing the temperature effects, is shown in Fig.8 (top), with the data compared with predictions for the sidereal effect only from the flyby Doppler shift data. As well that data is separated into two frequency bands (bottom), so that the sidereal effect is partially separated from the gravitational wave effect, *viz* 3-space wave/turbulence. Being 1st order in v/c it is easily determined that the space flow is from the southerly direction, as also reported in [1]. Miller reported the same sense, i.e. the flow is essentially from S to N, though using a 2nd order detector that is more difficult to determine. The frequency spectrum of this data is shown in Fig.7, revealing a fractal $1/f$ form. This implies the fractal structure of the 3-space indicated in Fig.9.

11 Optical Fibre RF Coaxial Cable Detector

An earlier 1st order in v/c gravitational wave detector design is shown in Fig.11, with some data shown in Fig.10. Only now is it known why that detector also worked, namely that there

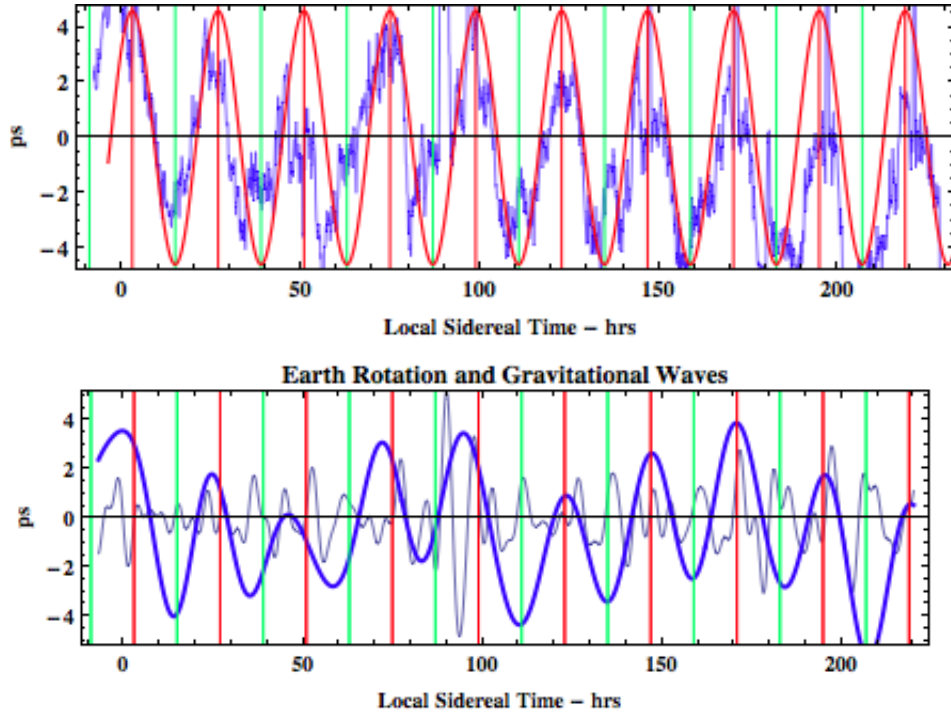


Fig. 8: Top: Travel time differences (ps) between the two coaxial cable circuits in Fig.6, orientated NS and horizontal, over 9 days (March 4-12, 2012, Adelaide) plotted against local sidereal time. Sinewave, with dynamic range 8.03ps, is prediction for sidereal effect from flyby Doppler shift data for RA=2.75^h (shown by red fiducial lines), Dec=-76.6°, and with speed 499.2km/s, see Table 2 of [9], also shown in from Fig.1. Data shows sidereal effect and significant wave/turbulence effects. Bottom: Data filtered into two frequency bands $3.4 \times 10^{-3}\text{mHz} < f < 0.018\text{mHz}$ ($81.4h > T > 15.3h$) and $0.018\text{mHz} < f < 0.067\text{mHz}$ ($15.3h > T > 4.14h$), showing more clearly the earth rotation sidereal effect (plus vlf waves) and the turbulence without the sidereal effect. Frequency spectrum of top data is shown in Fig.7.

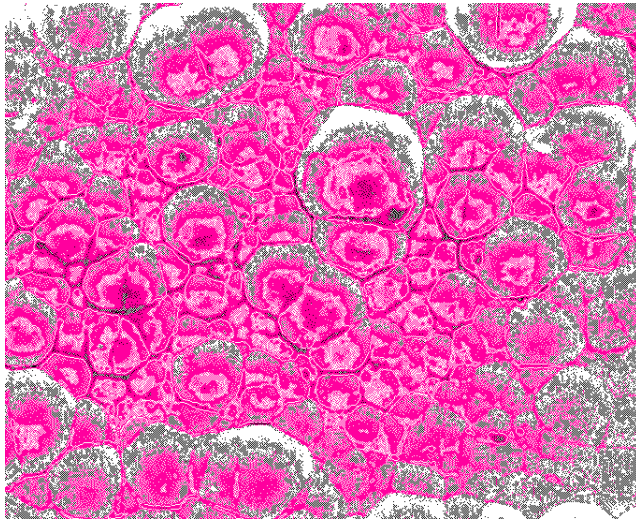


Fig. 9: Representation of the fractal wave data as a revealing the fractal textured structure of the 3-space, with cells of space having slightly different velocities, and continually changing, and moving wrt the earth with a speed of ~500km/s.

is a Fresnel drag effect in the optical fibres, but not in the RF coaxial cable. Then the travel time difference, measured at the DSO, is given by

$$\Delta t = \frac{2v \cos(\theta)L(n_1^2 - 1)}{c^2} + .. \quad (14)$$

where n_1 is the effective refractive index of the RF coaxial cable. Again the data is in remarkable agreement with the flyby determined v .

12 2nd Order in v/c Gas-Mode Detectors

It is important that the gas-mode 2nd order in v/c data from Michelson and Morley, 1887, and from Miller, 1925/26, be reviewed in the light of the recent experiments and flyby data. Shown in Fig.12 (top) is Miller data from September 16, 1925, 4^h 40' Local Sidereal Time (LST) - an average of data from 20 turns of the gas-mode Michelson interferometer. Plot and data after fitting and then subtracting both the temperature drift and Hicks effects from both, leaving the expected sinusoidal form. The error bars are determined as the rms error in this fitting procedure, and show how exceptionally small were the errors, and which agree with Miller's claim for the errors. Best result from the Michelson-Morley 1887 data - an average of 6

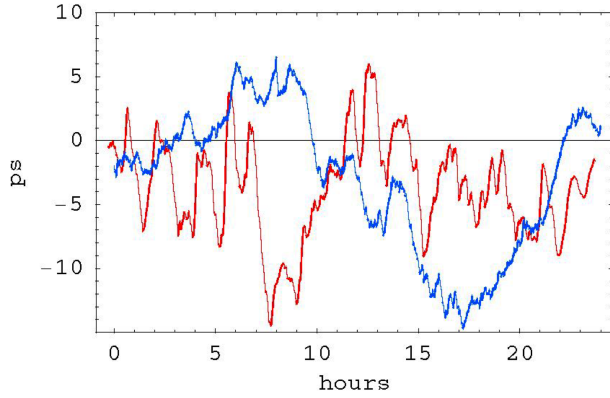


Fig. 10: Phase difference (ps), with arbitrary zero, versus local time data plots from the Optical Fibre - Coaxial Cable Detector, see Fig.11 and [1, 2], showing the sidereal time effect and significant wave/turbulence effects.. The plot (blue) with the most easily identified minimum at ~ 17 hrs local Adelaide time is from June 9, 2006, while the plot (red) with the minimum at ~ 8.5 hrs local time is from August 23, 2006. We see that the minimum has moved forward in time by approximately 8.5 hrs. The expected sidereal shift for this 65 day difference, without wave effects, is 4.3 hrs, to which must be added another ~ 1 h from the aberration effects shown in Fig1, giving 5.3hrs, in agreement with the data, considering that on individual days the min/max fluctuates by ± 2 hrs. This sidereal time shift is a critical test for the detector. From the flyby Doppler data we have for August RA= 5^h , Dec= -70° , and speed 478km/s, see Table 2 of [9], the predicted sidereal effect dynamic range to be 8.6ps, very close to that observed.

turns, at 7^h LST on July 11, 1887, is shown in Fig.12 (bottom). Again the rms error is remarkably small. In both cases the indicated speed is v_P - the 3-space speed projected onto the plane of the interferometer. The angle is the azimuth of the 3-space speed projection at the particular LST. Fig.13 shows speed fluctuations from day to day significantly exceed these errors, and reveal the existence of 3-space flow turbulence - i.e gravitational waves. The data shows considerable fluctuations, from hour to hour, and also day to day, as this is a composite day. The dashed curve shows the non-fluctuating best-fit sidereal effect variation over one day, as the earth rotates, causing the projection onto the plane of the interferometer of the velocity of the average direction of the space flow to change. The predicted projected sidereal speed variation for Mt Wilson is 251 to 415 km/s, using the Casinni flyby data and the STP air refractive index of $n = 1.00026$ appropriate atop Mt. Wilson, and the min/max occur at approximately 5hrs and 17hrs local sidereal time (Right Ascension). For the Michelson-Morley experiment in Cleveland the predicted projected sidereal speed variation is 239 to 465 km/s. Note that the Cassini flyby in August gives a RA= 5.15^h , close to the RA apparent in the above plot. The green data points, showing daily fluctuation bars, at 7^h and 13^h , are from the Michelson-Morley 1887 data, from averaging (excluding only the July 8 data for 7^h because it has poor S/N), and with same rms error analysis. The fiducial time

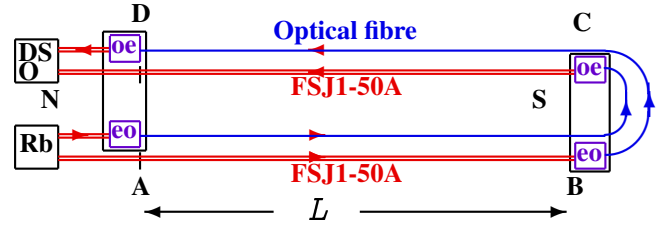


Fig. 11: Layout of the optical fibre - coaxial cable detector, with $L=5.0$ m. 10MHz RF signals come from the Rubidium atomic clock (Rb). The Electrical to Optical converters (EO) use the RF signals to modulate $1.3\mu\text{m}$ infrared signals that propagate through the single-mode optical fibres. The Optical to Electrical converters (OE) demodulate that signal and give the two RF signals that finally reach the Digital Storage Oscilloscope (DSO), which measures their phase difference. The key effects are that the propagation speeds through the coaxial cables and optical fibres respond differently to their absolute motion through space, with no Fresnel drag in the coaxial cables, and Fresnel drag effect in the optical fibres. Without this key difference this detector does not work.

lines are at 5^h and 17^h . The data indicates the presence of turbulence in the 3-space flow, i.e gravitational waves, being first seen in the Michelson-Morley experiment.

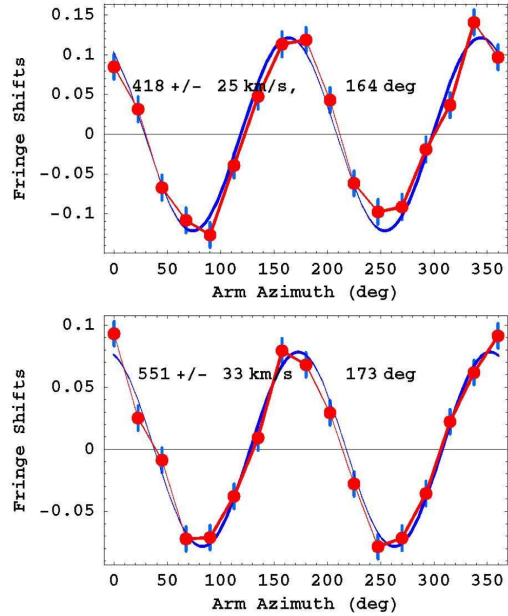


Fig. 12: Top: Typical Miller data from 1925/26 gas-mode Michelson interferometer, from 360° rotation. Bottom: Data from Michelson-Morley 1887 gas-mode interferometer, from 360° rotation.

13 Conclusions

The Dual RF Coaxial Cable Detector exploits the Fresnel drag anomaly in RF coaxial cables, *viz* the drag effect is absent in such cables, for reasons unknown, and this 1st order in v/c detector is compact, robust and uses one clock. This anomaly

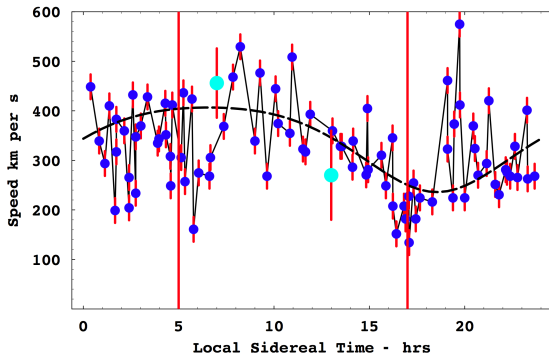


Fig. 13: Miller data for composite day in September 1925, and also showing Michelson-Morley 1887 July data at local sidereal times of 7^h and 13^h . The waved/turbulence effects are very evident, and comparable to data reported herein from the new detector.

now explains the operation of the Optical-Fibre - Coaxial Cable Detector, and permits a new calibration. These detectors have confirmed the absolute motion of the solar system and the gravitational wave effects seen in the earlier experiments of Michelson-Morley, Miller, DeWitte and Torr and Kolen. Most significantly these experiments agree with one another, and with the absolute motion velocity vector determined from spacecraft earth-flyby Doppler shifts. The observed significant wave/turbulence effects reveal that the so-called “gravitational waves” are easily detectable in small-scale laboratory detectors, and are considerably larger than those predicted by GR. These effects are not detectable in vacuum-mode Michelson terrestrial interferometers, nor by their analogue vacuum-mode resonant cavity experiments.

The new Dual RF Coaxial Cable Detector permits a detailed study and characterisation of the wave effects, and with the detector having the inclination equal to the local latitude the earth rotation effect may be removed, as the detector is then parallel to the earth’s spin axis, enabling a more accurate characterisation of the wave effects. The major discovery arising from these various results is that 3-space is directly detectable and has a fractal textured structure. This and numerous other effects are consistent with the dynamical theory for this 3-space. We are seeing the emergence of fundamentally new physics, with space being a non-geometrical dynamical system, and fractal down to the smallest scales describable by a classical velocity field, and below that by quantum foam dynamics [12]. Imperfect and incomplete is the geometrical model of space.

14 Acknowledgements

The Dual RF Coaxial Cable Detector is part of the Flinders University Gravitational Wave Detector Project. The DSO, Rb RF frequency source and coaxial cables were funded by an Australian Research Council Discovery Grant: *Development*

and Study of a New Theory of Gravity. Special thanks to CERN for donating the phase stabilised optical fibre, and to Fiber-Span for donating the optical-electrical converters. Thanks for support to Professor Warren Lawrance, Bill Drury, Professor Igor Bray, Finn Stokes and Dr David Brotherton.

References

- [1] Cahill R.T. *A New Light-Speed Anisotropy Experiment: Absolute Motion and Gravitational Waves*, *Progress in Physics*, v. 4, 73-92, 2006.
- [2] Cahill R.T. *Absolute Motion and Gravitational Wave Experiment Results*, Contribution to *Australian Institute of Physics National Congress*, Brisbane, Paper No. 202, 2006.
- [3] Cahill R.T. and Kitto K. *Michelson-Morley Experiments Revisited*, *Apeiron*, v. 10(2), 104-117, 2003.
- [4] Cahill R.T. *The Michelson and Morley 1887 Experiment and the Discovery of Absolute Motion*, *Progress in Physics*, v. 3, 25-29, 2005.
- [5] Miller D.C. *The Ether-Drift Experiment and the Determination of the Absolute Motion of the Earth*, *Rev. Mod. Phys.*, v. 5, 203-242, 1933.
- [6] Torr D.G. and Kolen P. *An Experiment to Measure Relative Variations in the One-Way Velocity of Light*, in *Precision Measurements and Fundamental Constants II*, Taylor B.N. and Phillips W.D. eds. *Natl. Bur. Stand. (U.S.), Spec. Pub.*, 617, 675-679, 1984.
- [7] Cahill R.T. *The Roland De Witte 1991 Experiment*, *Progress in Physics*, v. 3, 60-65, 2006.
- [8] Anderson J.D., Campbell J.K., Ekelund J.E., Ellis J. and Jordan J.F. *Anomalous Orbital-Energy Changes Observed during Spacecraft Flybys of Earth*, *Phys. Rev. Lett.*, v. 100, 091102, 2008.
- [9] Cahill R.T. *Combining NASA/JPL One-Way Optical-fibre Light-Speed Data with Spacecraft Earth-Flyby Doppler-Shift Data to Characterise 3-Space Flow*, *Progress in Physics*, v. 4, 50-64, 2009.
- [10] Cahill R.T. *Unravelling Lorentz Covariance and the Spacetime Formalism*, *Progress in Physics*, v. 4, 19-24, 2008.
- [11] Cahill R.T. and Stokes F. *Correlated Detection of sub-mHz Gravitational Waves by Two Optical-fibre Interferometers*, *Progress in Physics*, v. 2, 103-110, 2008.
- [12] Cahill R.T. *Process Physics: From Information Theory to Quantum Space and Matter*, *Nova Science Pub.*, New York, 2005.
- [13] Cahill R.T. and Brotherton D., *Experimental Investigation of the Fresnel Drag Effect in RF Coaxial Cables*, *Progress in Physics*, v. 1, 43-48, 2011.